

A Comparative Study on the Molecular Structures and Vibrational Spectra of 2-, 3- and 4-Cyanopyridines by Density Functional Theory.

Yunusa Umar

Department of Chemical and Process Engineering Technology, Jubail Industrial College
POBox 10099, Jubail Industrial City- 31961, Saudi Arabia.

Abstract: The optimized molecular structures, harmonic vibrational wavenumbers, and corresponding vibrational assignments of 2-, 3- and 4-cyanopyridines have been calculated using Gaussian 03 set of quantum chemistry code. Calculations were carried out at Becke-3-Lee-Yang-Parr (B3LYP) density functional theory (DFT) level using the standard 6-311++G(d,p) basis set. The geometrical parameters, thermodynamic parameters, highest occupied and lowest unoccupied molecular orbitals (HOMO and LUMO), Infrared intensities, Raman activities and molecular electrostatic potentials results are reported. Reliable vibrational assignments have been made on the basis of Potential Energy Distribution (PED) using VEDA4 program. Theoretical results have been successfully compared with the available experimental data.

Keywords: Cyanopyridine, DFT, PED, Vibrational spectra,

I. Introduction

The three isomeric compounds 2-cyanopyridine (2-CNP), 3-cyanopyridine (3-CNP) and 4-cyanopyridine (4-CNP) which are also known as picolinonitrile, nicononitrile and isonicotinic nitrile, respectively contain cyano group (CN) substituted at ortho, meta, para positions of pyridine ring. These cyanopyridines have applications in pharmaceutical [1-3], corrosion inhibition [4], catalysis [4, 5], synthesis of organic compounds and organometallic complexes [7-10]. Cyanopyridines are widely used as a starting material and intermediates for the synthesis of high valued carboxylic acids and amides. For example, 3-CNP is a value intermediate in the synthesis of nicotinic acid (vitamin B₃, niacin) and nicotinamide (drugs) [1, 2, 11-15]. Since nitrogen of both cyano group and the pyridine ring of cyanopyridines are capable of coordinating with metal ions, these compounds are also used in the synthesis of organometallic complexes [7-10].

Green et al. [16] recorded the vibrational infrared and Raman spectra of the title compounds and suggested assignments of the observed vibrational wavenumbers. Oliver et al. [17] investigated the configuration of 4-CNP on Au (111) electrodes in percholate solution by in situ visible-infrared sum frequency generation. Laing et al. [18] reported crystal structure of 4-CNP from three dimensional single X-ray data collected by standard film techniques. On the other hand, the crystal structures of 2- and 3-cyanopyridines have been reported on the basis of the low temperature X-ray single crystal experiments [19].

Despite the wide applications of cyanopyridines, to the best of our knowledge, there is no detailed theoretical study present in the literature about the structural and vibrational properties of these molecules. Such studies will not only aid in making definitive assignments of the fundamental normal modes and in clarifying experimental data but will also be helpful in context of further studies of these molecules. The B3LYP density functional theory calculations exhibit good performance on the molecular geometries and vibrational properties of organic compounds [20-25]. Thus, the aim of this work is to take advantage of the quantum-mechanical calculations to carry out systematic study on the molecular structure and vibrational spectra which will give depth insight in understanding the properties of the title molecules and aid in clarifying and complementing available experimental data. This paper will reveal additional quantitative chemical knowledge and detailed insight about the molecular structure, thermodynamic properties, vibrational spectra and assignments of vibrational mode of these compounds.

II. Computational Methods

Gaussian 03 program package [26] was used to optimize the structures, predict energies, and calculate thermodynamic parameters, atomic charges and vibrational wavenumbers of 2-CNP, 3-CNP and 4-CNP. Computations were performed using Density Functional Theory (DFT) adopting Becke's three-parameter exchange functional [28] combined with Lee-Yang-Parr [29] correlation functional (B3LYP) methods. The standard 6-311++G(d,p) basis set was used for all the atoms to carry out the calculations utilizing the C_s symmetry of 2-CNP and 3-CNP and C_{2v} symmetry of the symmetrical 4-CNP. The infrared data are reported, and each of the vibrational modes was visually confirmed by Gauss-View program [30]. The VEDA4 program

[31] was used to characterize the normal vibrational modes on the basis of Potential Energy Distribution. The wavenumbers and intensities obtained from the computations were used to simulate infrared spectra. In addition, the highest occupied molecular orbital (HOMO) and lowest unoccupied molecular orbital (LUMO) energy values, HOMO-LUMO energy gaps, molecular electrostatic potentials (MEP) for the three isomeric compounds were calculated at B3LYP/6-311++G(d,p) level of theory.

III. Result and Discussion

3.1 Molecular Geometry

The optimized molecular structures along with the numbering of atoms of 2-, 3- and 4-cyanopyridines calculated at B3LYP/6-311++G(d,p) level of theory are given in Fig. 1. The geometrical parameters (bond lengths and bond angles) corresponding to the optimized geometries of the title molecules are given in Table 1 along with the X-ray experiment data [18, 19]. Generally, most of the optimized bond lengths are slightly longer than the experimental values, and the bond angles are slightly different from the experimental ones. This is expected because, one isolated molecule is considered in theoretical gas phase calculation, whereas packed molecules are considered in solid phase during the experimental measurement. However, the calculated geometric parameters are in good agreement with the experimental results. To be specific, the root meansquare (RMS) errors are 0.017 Å, 0.009 Å and 0.012 Å for the bond lengths of 2-CNP, 3-CNP and 4-CNP respectively; while the RMS errors for the bond angles are found to be 0.99°, 0.54° and 0.61° for the 2-CNP, 3-CNP and 4-CNP respectively. In addition, the calculation also shows that there are no systematic and significant changes in the geometric parameters of the three molecules. The position of the cyano group has no significant effect of the geometric parameters of the molecules. The C≡N bond lengths of the three molecules are calculated to be around 1.155 Å, and the average bond distance between the pyridine ring and the cyano group (C-CN) for the three molecules is 1.435 Å. The average values for the pyridine ring C-C and C-H bond lengths are 1.379 Å and 1.084 Å; 1.397 Å and 1.084 Å; 1.382 Å and 1.084 Å in 2-CNP, 3-CNP and 4-CNP respectively. The bond lengths and the bond angles of the three isomers are comparable to the values found in 2-, 3- and 4-formylpyridines [21].

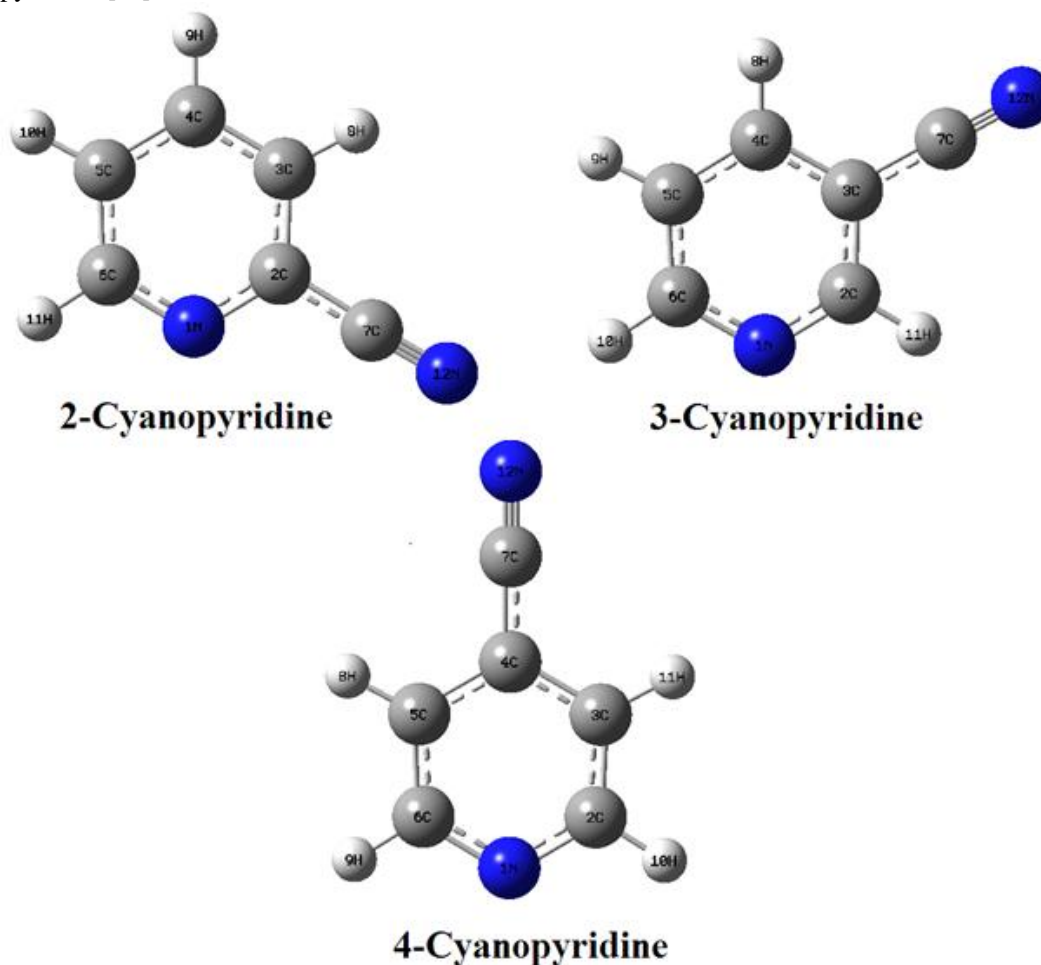


Figure 1. Optimized molecular structure along with atom numbering of 2-, 3- and 4- cyanopyridines.

Table 1: Experimental and calculated optimized geometrical parameters for 2-, 3- and 4-cyanopyridines.

| Geometry Parameter ^a | 2-Cyanopyridine | | 3-Cyanopyridine | | 4-Cyanopyridine | |
|---|------------------------|------------------------|------------------------|------------------------|-------------------------|-------------------------|
| | Expt ^b | Calc | Expt ^b | Calc | Expt ^c | Calc |
| Bond lengths(Å) | | | | | | |
| N ₁ -C ₂ | 1.344 | 1.340 | 1.335 | 1.33 | 1.331 | 1.336 |
| C ₂ -C ₃ | 1.374 | 1.340 | 1.392 | 1.404 | 1.383 | 1.392 |
| C ₃ -C ₄ | 1.368 | 1.390 | 1.386 | 1.401 | 1.381 | 1.399 |
| C ₄ -C ₅ | 1.376 | 1.391 | 1.376 | 1.388 | 1.381 | 1.399 |
| C ₅ -C ₆ | 1.378 | 1.396 | 1.384 | 1.395 | 1.383 | 1.392 |
| C ₆ -N ₁ | 1.340 | 1.333 | 1.337 | 1.337 | 1.331 | 1.336 |
| C _n -C ₇ | 1.448(C ₂) | 1.442(C ₂) | 1.430(C ₃) | 1.429(C ₃) | 1.439 (C ₄) | 1.433 (C ₄) |
| C ₇ ≡N ₁₂ | 1.145 | 1.154 | 1.150 | 1.155 | 1.137 | 1.155 |
| C-H ₈ | -(C ₂) | 1.083 | -(C ₂) | 1.085(C ₂) | -(C ₂) | 1.086(C ₂) |
| C-H ₉ | -(C ₄) | 1.084 | -(C ₄) | 1.083(C ₄) | -(C ₃) | 1.082(C ₃) |
| C ₅ -H ₁₀ | - | 1.083 | - | 1.083 | - | 1.082 |
| C ₆ -H ₁₁ | - | 1.086 | - | 1.086 | - | 1.086 |
| Bond Angles(°) | | | | | | |
| N ₁ C ₂ C ₃ | 124.8 | 123.8 | 122.5 | 123.1 | 123.9 | 123.7 |
| C ₂ C ₃ C ₄ | 118.3 | 118.0 | 119.5 | 118.5 | 117.5 | 118.1 |
| C ₃ C ₄ C ₅ | 118.9 | 118.8 | 118.1 | 118.3 | 120.0 | 118.7 |
| C ₄ C ₅ C ₆ | 118.7 | 118.6 | 118.8 | 118.7 | 117.5 | 118.1 |
| C ₅ C ₆ N ₁ | 124.1 | 123.6 | 123.9 | 123.6 | 123.9 | 123.7 |
| C ₆ N ₁ C ₂ | 115.2 | 117.2 | 117.2 | 117.8 | 117.3 | 117.6 |
| C _n C ₇ N ₁₂ | 179.2(C ₂) | 178.0(C ₂) | 179.5(C ₃) | 179.9(C ₃) | 180.0(C ₄) | 180.0(C ₄) |

^aThe atom numbering is given in Fig.1; ^b Taken from Ref. [19]; ^c Taken from Ref. [18].

3.2 Vibrational Spectra

Optimized structural parameters were used to compute the vibrational wavenumbers for the three cyanopyridines at B3LYP/6-311++G(d,p) level of theory. Since DFT hybrid B3LYP functional tends to overestimate the fundamental modes, the calculated vibrational wavenumbers are usually higher than the observed vibrational modes, and the differences are accounted for by using scaling factor. Therefore, the calculated vibrational wavenumbers are scaled with 0.955 and 0.977 for the vibrational wavenumbers above and below 1800 cm⁻¹ respectively [32]. Tables 2-4 present the calculated vibrational wavenumbers, IR intensities and Raman activities along with assignments of vibrational modes for the three cyanopyridines. Each of these Tables gives the observed infrared wavenumbers [16] of the three molecules for comparison. The assignment of the fundamental vibrational modes is proposed on the basis of Potential Energy Distribution (PED) using VEDA 4 program and the animation option of Gauss View graphical interface of Gaussian program.

From the optimized structures, it is observed that 2-CNP and 3-CNP have C_s point group symmetry, while 4-CNP has C_{2v} point group symmetry. The three isomers of the cyanopyridine are composed of 12 atoms. Thus, the calculations result in thirty IR fundamental vibrations that belong to irreducible representations $\Gamma_{\text{vib}} = 21 A' + 9 A''$ of the C_s point group of 2-CNP and 3- CNP, and $\Gamma_{\text{vib}} = 11A_1 + 3A_2 + 6B_1 + 10B_2$ of the C_{2v} point group of 4-CNP. The absence of imaginary wavenumbers in the calculated vibrational spectrum confirms that the optimized structures correspond to the minimum energy. The A₁ and B₂ irreducible representations correspond to stretching, ring deformation, and in-plane bending vibrations, while A₂ and B₁ correspond to ring, torsion and out of plane bending vibrations. Similarly, the A' and A'' irreducible representations correspond to in-plane and out-of-plane modes respectively. The B3LYP/6-311++G(d,p) calculations give the value of C≡N stretching modes at 2289 cm⁻¹, 2258 cm⁻¹ and 2263 cm⁻¹ for 2-CNP, 3-CNP and 4-CNP respectively.

In order to investigate the performance of the theoretical calculation, the root mean square (RMS) error between the calculated and observed wavenumbers were calculated using the following equation (1).

$$\text{RMS} = \sqrt{\frac{\sum_i^n (v_i^{\text{calc}} - v_i^{\text{exp}})^2}{n - 1}} \text{-----} 1$$

The RMS errors of the observed IR bands are found to be 16 cm⁻¹, 15 cm⁻¹ and 13 cm⁻¹ for 2-CNP, 3-CNP and 4-CNP respectively. Similarly, the correlation values obtained from the graph of observed wavenumbers against calculated wavenumbers are found to be 0.9996, 0.9997 and 0.9998 for 2-CNP, 3-CNP and 4-CNP respectively. Both RMS and correlation values clearly show the very good agreement between observed and calculated vibrational wavenumbers, which indicates that the B3LYP/6-311++G(d,p) calculation

is reliable for the prediction of vibrational spectra. The vibrational wavenumbers and the corresponding intensities obtained from B3LYP/6-311++G(d,p) calculations were used to simulate the infrared and Raman spectra of the studied molecules. For simulation, pure Lorentzian band shape with a bandwidth of full width and half maximum (FWHM) of 10 cm^{-1} was used to plot the calculated IR and Raman spectra. The simulated IR and Raman spectra of the three molecules are presented in Figs. 2 and 3. These figures clearly show the difference in spectral characteristics of the title molecules. Calculated Raman activities (S_i) were converted to relative Raman intensities (I_i) using the following equation (2) derived from the intensity theory of Raman scattering [33, 34].

$$I_i = \frac{f(v_0 - v_i)^4 S_i}{v_i [1 - \exp(-\frac{hcv_i}{kT})]} \quad \text{---2}$$

Where v_0 is the laser exciting wavenumber in cm^{-1} , v_i is the vibrational wavenumber of the i th normal mode, and f is a suitable common normalization factor for all peak intensities, 10^{-4} . h , k , c and T are Planck and Boltzman constants, speed of light and temperature in Kelvin, respectively.

Table 2: Experimental and corresponding scaled theoretical vibrational wavenumbers (cm^{-1}) of 2-cyanopyridine.

| No. | Sym. | Expt ^a | v ^b | I _{IR} ^c | I _R ^c | Assignment (PED ≥ 10%) |
|-----------------|------|-------------------|----------------|------------------------------|-----------------------------|---------------------------------|
| v ₁ | A' | 3088 | 3061 | 1.66 | 183.43 | υCH (95) |
| v ₂ | A' | 3064 | 3053 | 8.04 | 112.96 | υCH (96) |
| v ₃ | A' | 3005 | 3038 | 3.84 | 83.51 | υCH (92) |
| v ₄ | A' | - | 3020 | 10.37 | 98.66 | υCH (92) |
| v ₅ | A' | 2238 | 2289 | 6.65 | 411.15 | υCN(90) + υCC(10) |
| v ₆ | A' | 1580 | 1583 | 19.96 | 84.75 | υCC (57) + δHCC(13) |
| v ₇ | A' | 1574 | 1571 | 20.07 | 7.76 | υCC (58) + δHCC(14) |
| v ₈ | A' | 1462 | 1460 | 21.00 | 4.23 | υCC (34) + δHCC(50) |
| v ₉ | A' | 1432 | 1424 | 17.92 | 7.18 | δHCC(57) |
| v ₁₀ | A' | 1295 | 1288 | 1.78 | 3.17 | υCC(33) + δHCC(56) |
| v ₁₁ | A' | 1248 | 1263 | 4.59 | 0.45 | υCC(79) |
| v ₁₂ | A' | 1207 | 1206 | 3.14 | 51.01 | υCC(39) + δCNC(25) + δHCC(12) |
| v ₁₃ | A' | 1155 | 1147 | 2.35 | 3.98 | υCC(13) + δHCC(73) |
| v ₁₄ | A' | 1091 | 1091 | 2.65 | 1.74 | υCC(37) + δHCC(35) |
| v ₁₅ | A' | 1045 | 1041 | 5.36 | 17.37 | υCC(44) + δHCC(12) + δCCC(24) |
| v ₁₆ | A'' | 992 | 994 | 0.01 | 0.20 | τHCCC(67) + τCCCN(13) |
| v ₁₇ | A' | 981 | 985 | 6.52 | 36.15 | υCC(41) + δCCC(44) |
| v ₁₈ | A'' | 933 | 964 | 0.56 | 0.05 | τHCCC(81) + τCNCC(10) |
| v ₁₉ | A'' | 896 | 895 | 0.58 | 0.00 | τHCCC(82) |
| v ₂₀ | A'' | 777 | 783 | 42.77 | 0.95 | τHCCC(53) + τCNCC(37) |
| v ₂₁ | A' | - | 775 | 3.73 | 9.32 | υCC(24) + δCNC(56) |
| v ₂₂ | A'' | 734 | 735 | 14.25 | 0.16 | τHCCC(47) + τCNCC(46) |
| v ₂₃ | A' | 632 | 631 | 1.30 | 2.58 | δCCC(67) + δCCN (11) + δCNC(10) |
| v ₂₄ | A'' | 553 | 562 | 11.17 | 2.47 | τHCCC(10) + τNCCC(34) + |
| v ₂₅ | A' | - | 558 | 2.88 | 3.34 | δCCN(79) |
| v ₂₆ | A' | 477 | 474 | 0.40 | 3.98 | υCC(32) + δCNC(49) |
| v ₂₇ | A'' | 403 | 404 | 5.49 | 0.30 | τHCCC (12) + τCNCC(80) |
| v ₂₈ | A'' | 362 | 362 | 0.74 | 1.48 | τNCCC (41) + τCCCN (44) |
| v ₂₉ | A' | - | 169 | 2.55 | 3.41 | δCCN(85) + δCCN(10) |
| v ₃₀ | A'' | - | 138 | 0.50 | 0.31 | τNCCC(19) + τCCNC(65) |

^aTaken from Ref. [21];

^bScaled IR vibrational wavenumbers (scaled with 0.955 above 1800 cm^{-1} and 0.977 under 1800 cm^{-1})

^c I_{IR} , calculated infrared intensities in km mol^{-1} ; I_R , calculated Raman intensities in $\text{\AA}^4\text{ amu}^{-1}$.

Table 3: Experimental and corresponding scaled theoretical vibrational wavenumbers (cm^{-1}) of 3-cyanopyridine.

| No. | Sym. | Expt ^a | ν^b | I_{IR}^c | I_{R}^c | Assignment (PED $\geq 10\%$) |
|-----------------|------|-------------------|---------|-------------------|------------------|---|
| v ₁ | A' | 3088 | 3059 | 4.15 | 168.16 | ν_{CH} (98) |
| v ₂ | A' | 3050 | 3045 | 3.80 | 84.27 | ν_{CH} (95) |
| v ₃ | A' | 3036 | 3027 | 3.41 | 76.69 | ν_{CH} (96) |
| v ₄ | A' | 3012 | 3056 | 11.56 | 109.1 | ν_{CH} (92) |
| v ₅ | A' | 2237 | 2258 | 28.39 | 418.48 | ν_{CN} (89) + ν_{CC} (12) |
| v ₆ | A' | 1586 | 1590 | 20.18 | 88.98 | ν_{CC} (56) + δ_{HCC} (14) |
| v ₇ | A' | 1562 | 1561 | 13.56 | 7.29 | ν_{CC} (60) + δ_{HCN} (10) |
| v ₈ | A' | 1471 | 1470 | 13.00 | 3.66 | ν_{CC} (23) + δ_{HCC} (46) |
| v ₉ | A' | 1415 | 1412 | 24.22 | 2.52 | δ_{HCN} (43) + δ_{CNC} (10) |
| v ₁₀ | A' | 1333 | 1332 | 1.68 | 1.03 | δ_{HCN} (86) |
| v ₁₁ | A' | 1234 | 1249 | 0.26 | 2.38 | ν_{CC} (80) |
| v ₁₂ | A' | 1211 | 1206 | 4.16 | 19.90 | ν_{CC} (37) + δ_{HCC} (25) |
| v ₁₃ | A' | 1185 | 1188 | 5.21 | 25.54 | ν_{CC} (40) + δ_{HCN} (11) + δ_{HCC} (11) |
| v ₁₄ | A' | 1122 | 1116 | 5.01 | 3.16 | ν_{CC} (21) + δ_{HCC} (41) |
| v ₁₅ | A' | 1033 | 1036 | 0.71 | 33.13 | ν_{CC} (66) + δ_{HCC} (13) |
| v ₁₆ | A'' | 1023 | 1015 | 11.16 | 20.83 | δ_{CNC} (63) |
| v ₁₇ | A' | 958 | 982 | 0.00 | 0.04 | τ_{HCCC} (68) + τ_{CCCN} (20) |
| v ₁₈ | A'' | 926 | 956 | 1.32 | 0.07 | τ_{HCCC} (79) |
| v ₁₉ | A'' | 902 | 925 | 0.91 | 0.25 | τ_{HCNC} (67) + τ_{CNCC} (14) |
| v ₂₀ | A'' | 803 | 800 | 26.03 | 0.80 | τ_{HCCN} (69) + τ_{CCNC} (17) |
| v ₂₁ | A' | 776 | 774 | 0.42 | 10.33 | ν_{CC} (27) + δ_{CCN} (60) |
| v ₂₂ | A'' | 701 | 699 | 31.22 | 0.23 | τ_{HCNC} (13) + τ_{HCNC} (19) + τ_{HCCC} (11) |
| v ₂₃ | A' | 624 | 625 | 4.27 | 3.69 | δ_{CCC} (16) + δ_{CNC} (67) |
| v ₂₄ | A'' | 548 | 565 | 2.84 | 2.33 | τ_{NCCC} (45) + τ_{CCCC} (36) |
| v ₂₅ | A' | 542 | 553 | 0.37 | 1.85 | δ_{CCN} (76) |
| v ₂₆ | A' | 470 | 467 | 0.29 | 5.87 | ν_{CC} (28) + δ_{CCC} (32) + δ_{CNC} (16) |
| v ₂₇ | A'' | 397 | 399 | 4.58 | 0.68 | τ_{CNCC} (78) |
| v ₂₈ | A'' | 355 | 356 | 0.50 | 1.45 | τ_{NCCC} (25) + τ_{CCCN} (56) |
| v ₂₉ | A' | - | 164 | 6.53 | 3.71 | δ_{CCN} (88) |
| v ₃₀ | A'' | - | 146 | 3.60 | 0.32 | τ_{NCCC} (22) + τ_{CCCN} (16) + τ_{CCCC} (47) |

^aTaken from Ref. [21].

^bScaled IR vibrational wavenumbers (scaled with 0.955 above 1800 cm^{-1} and 0.977 under 1800 cm^{-1})

^c I_{IR} , calculated infrared intensities in km mol^{-1} ; I_{R} , calculated Raman intensities in $\text{\AA}^4 \text{ amu}^{-1}$.

Table 4: Experimental and corresponding scaled theoretical vibrational wavenumbers (cm^{-1}) of 4-cyanopyridine.

| No. | Sym. | Expt ^a | ν^b | I_{IR}^c | I_R^c | Assignment (PED \geq 10%) |
|-----------------|----------------|-------------------|---------|------------|---------|--|
| v ₁ | A ₁ | 3082 | 3061 | 0.11 | 200.51 | ν_{CH} (95) |
| v ₂ | B ₂ | 3066 | 3061 | 3.22 | 17.45 | ν_{CH} (97) |
| v ₃ | A ₁ | 3051 | 3019 | 2.95 | 123.00 | ν_{CH} (96) |
| v ₄ | B ₂ | 3031 | 3054 | 21.63 | 102.90 | ν_{CH} (97) |
| v ₅ | A ₁ | 2238 | 2263 | 12.36 | 375.74 | ν_{CN} (89) + ν_{CC} (10) |
| v ₆ | A ₁ | 1591 | 1591 | 30.87 | 61.28 | ν_{CC} (52) + δ_{CCC} (12) + δ_{HCN} (20) |
| v ₇ | B ₂ | 1552 | 1550 | 21.47 | 1.22 | ν_{CC} (75) + δ_{CCN} (12) |
| v ₈ | A ₁ | 1487 | 1485 | 2.50 | 5.28 | τ_{HCN} (61) + δ_{CCN} (19) |
| v ₉ | B ₂ | 1406 | 1407 | 19.91 | 1.39 | ν_{CC} (28) + δ_{HCN} (62) |
| v ₁₀ | B ₂ | 1324 | 1322 | 0.48 | 3.90 | δ_{HCC} (74) |
| v ₁₁ | B ₂ | 1244 | 1237 | 4.38 | 6.75 | ν_{CN} (80) |
| v ₁₂ | A ₁ | 1219 | 1217 | 4.98 | 3.61 | ν_{CC} (37) + δ_{HCN} (56) |
| v ₁₃ | A ₁ | 1194 | 1192 | 0.56 | 55.61 | ν_{CC} (37) + δ_{HCN} (15) + ν_{CC} (21) |
| v ₁₄ | B ₂ | 1081 | 1083 | 0.85 | 0.18 | ν_{CC} (60) + δ_{HCN} (25) |
| v ₁₅ | A ₁ | 1067 | 1067 | 3.53 | 1.20 | ν_{CN} (16) + δ_{HCC} (32) + δ_{CCN} (41) |
| v ₁₆ | A ₁ | 989 | 985 | 3.36 | 35.66 | ν_{CN} (60) + δ_{CCN} (30) |
| v ₁₇ | A ₂ | 961 | 980 | 0.00 | 0.07 | τ_{HCNC} (87) + τ_{CCNC} (10) |
| v ₁₈ | B ₁ | 932 | 960 | 0.73 | 0.02 | τ_{HCNC} (72) + τ_{CCNC} (16) |
| v ₁₉ | A ₂ | 865 | 865 | 0.00 | 0.01 | τ_{HCNC} (99) |
| v ₂₀ | B ₁ | 817 | 820 | 42.83 | 0.74 | τ_{HCNC} (67) + τ_{CCNC} (64) |
| v ₂₁ | A ₁ | 772 | 763 | 14.45 | 10.19 | ν_{CC} (25) + δ_{CCC} (59) |
| v ₂₂ | B ₁ | 710 | 731 | 0.03 | 0.02 | τ_{HCNC} (24) + τ_{CCNC} (66) |
| v ₂₃ | B ₂ | 663 | 669 | 0.10 | 5.15 | δ_{CCN} (79) |
| v ₂₄ | B ₁ | 560 | 573 | 22.8 | 2.94 | τ_{HCNC} (22) + τ_{NCCC} (26) + τ_{CCCC} (22) |
| v ₂₅ | B ₂ | - | 556 | 0.05 | 2.27 | δ_{CCN} (65) + τ_{NCCC} (15) |
| v ₂₆ | A ₁ | 454 | 449 | 0.81 | 4.94 | ν_{CC} (13) + δ_{CCC} (65) |
| v ₂₇ | B ₁ | 374 | 382 | 0.92 | 0.89 | τ_{NCCC} (20) + τ_{CCNC} (54) |
| v ₂₈ | A ₂ | - | 369 | 0.00 | 0.75 | τ_{HCNC} (11) + τ_{CCNC} (83) |
| v ₂₉ | B ₂ | 166 | 165 | 7.96 | 4.17 | δ_{CCN} (75) + τ_{NCCC} (15) |
| v ₃₀ | B ₁ | 147 | 143 | 9.14 | 0.02 | τ_{NCCC} (20) + τ_{CCCC} (56) + τ_{CCNC} (10) |

^aTaken from Ref. [21].; ^b Scaled IR vibrational wavenumbers (scaled with 0.955 above 1800 cm^{-1} and 0.977 under 1800 cm^{-1})

^c I_{IR} , calculated infrared intensities in km mol^{-1} ; I_R , calculated Raman intensities in $\text{\AA}^4 \text{amu}^{-1}$.

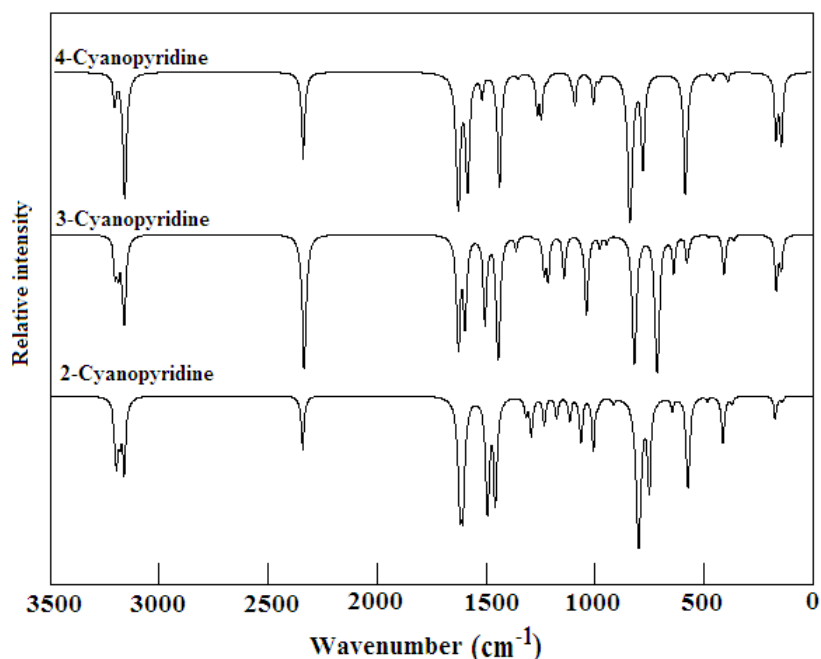


Figure 2: Simulated vibrational infrared spectra of 2-, 3- and 4-cyanopyridine.

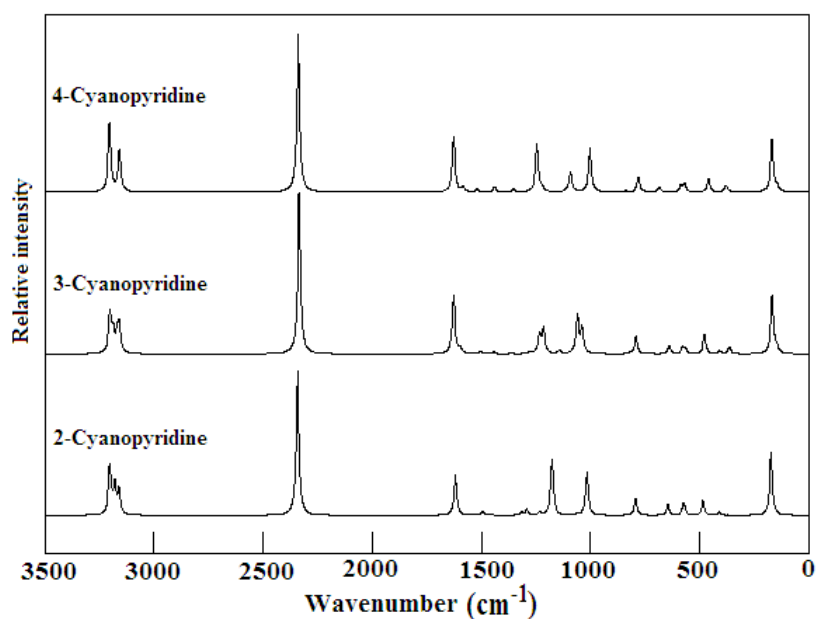


Figure 3: Simulated vibrational Raman spectra of 2-, 3- and 4-cyanopyridine.

3.3 Thermodynamic parameters and HOMO-LUMO analysis

Several thermodynamic parameters, rotational constants and dipole moments for 2-CNP, 3-CNP and 4-CNP calculated at B3LYP/6-311++G(d,p) are presented in Table 5. The zero point energy, SCF energy, entropy, and heat capacity for the title molecules are obtained from the theoretical harmonic frequency calculations. The relative stabilization energy which is the energy differences between the cyanopyridine isomers, shows that both 2-CNP and 4-CNP have higher energy than 3-CNP, while 2-CNP has the highest energy and the 3-CNP has the least energy. The same trend was reported for formylpyridines [21] where the total energy order was found to be 3-formylpyridine < 4-formylpyridine < 2-formylpyridine. These energy differences of the ortho, meta and para isomers of substituted pyridines could be explained in terms of the electronic and steric effects. The observed rotational constants and dipole moments [35] obtained from microwave spectra of the three cyanopyridines are also presented in Table 5. A comparison of the calculated rotational constants and dipole moments with the experimental values reveals that the results obtained from B3LYP/6-311++G(d,p) are in very good agreement with experimental observations.

Table 5: The calculated thermodynamics parameters 2-CNP, 3-CNP and 4-CNP

| Parameter | 2-CNP | 3-CNP | 4-CNP |
|---|--------------|--------------|--------------|
| SCF Energy (Hartree) | -340.613490 | -340.615286 | -340.613992 |
| Relative Stabilization Energy (K cal mol ⁻¹) | 1.13 | 0.00 | 0.81 |
| Total Thermal Energy, E _{total} (K cal mol ⁻¹) | 58.254 | 58.333 | 58.317 |
| Heat capacity at const. volume, C _v (cal mol ⁻¹ K ⁻¹) | 22.305 | 22.300 | 22.271 |
| Entropy, S (cal mol ⁻¹ K ⁻¹) | 78.193 | 78.267 | 76.857 |
| Vibrational energy, E _{vib} (K cal mol ⁻¹) | 56.477 | 56.561 | 56.540 |
| Zero point vibrational energy, E ₀ (K cal mol ⁻¹) | 54.494 | 54.568 | 54.554 |
| Rotational Constant (MHz)* | | | |
| A | 5860 (5837) | 5846 (5823) | 6016 (6000) |
| B | 1600 (1598) | 1573 (1571) | 1544 (1541) |
| C | 1257 (1254) | 1239 (1237) | 1229 (1226) |
| Dipole moment (Debye)* | 5.950 (5.78) | 4.032 (3.66) | 2.008 (1.96) |

*Values in bracket are experiment values taken from Ref. [35].

The highest occupied molecular orbital (HOMO) and the lowest unoccupied molecular orbital (LUMO) and their properties are very useful for predicting the most reactive position in π -electron systems. They are also useful in explaining several types of reactions in conjugated system [36]. The HOMO represents the ability to donate an electron, while the LUMO represents the ability to accept an electron. Thus, the energy of the HOMO is directly related to the ionization potential, while the LUMO energy is directly related to electron affinity, and the HOMO-LUMO energy gap is related to the molecular chemical stability. A molecule with a small HOMO-LUMO energy gap is more polarizable and is generally associated with high chemical reactivity [37, 38]. The HOMO and LUMO of the title molecules were calculated at B3LYP/6-311++G(d,p) level of theory. The 3D plots generated from the calculations are illustrated in Fig. 4, while the HOMO and LUMO energies and the HOMO-LUMO energy gaps are presented in Table 6. In addition, the HOMO and LUMO energy values are used to calculate global chemical reactivity descriptors such as ionization potential (I), electron affinity (A), electronegativity (χ), chemical hardness (η), chemical softness (S), chemical potential (μ), electrophilicity index (ω). The results are summarized in Table 6. The HOMO and LUMO are delocalized over the entire molecules of 3-CNP and 4-CNP, while those of the 2-CNP are localized on a portion of the pyridine ring of the molecule. The HOMO and LUMO energy values reflect the relative chemical stability and biological activity of the title compounds.

Table 6: The calculated HOMO and LUMO energies, HOMO-LUMO energy gap, ionization potential, electron affinity, electronegativity, chemical hardness, chemical potential, chemical softness and electrophilicity index of 2-, 3-, and 4-cyano pyridines.

| Property | 2-CNP | 3-CNP | 4-CNP |
|---|----------|----------|----------|
| E _{HOMO} (hartress) | -0.29314 | -0.29217 | -0.29179 |
| E _{LUMO} (hartress) | -0.0236 | -0.08264 | -0.09124 |
| E _{HOMO} (eV) | -7.9765 | -7.9502 | -7.9398 |
| E _{LUMO} (eV) | -0.6422 | -2.2487 | -2.4827 |
| ΔE = E _{HOMO} - E _{LUMO} gap (eV) | 7.3344 | 5.7015 | 5.4571 |
| Ionization potentials, I = - E _{HOMO} (eV) | 7.9765 | 7.9502 | 7.9398 |
| Electron affinity, A = - E _{LUMO} (eV) | 0.6422 | 2.2487 | 2.4827 |
| Electronegativity, χ = (I + A)/2 (eV) | 4.3094 | 5.0994 | 5.2113 |
| Chemical hardness, η = (I - A)/2 (eV) | 3.6672 | 2.8507 | 2.7286 |
| Chemical potential, μ = -(I + A)/2 (eV) | -4.3094 | -5.0994 | -5.2113 |
| Chemical softness, S = 1/(2 η) (eV ⁻¹) | 0.1363 | 0.1754 | 0.1832 |
| Electrophilicity index, ω = $\mu^2/2\eta$ (eV) | 2.5320 | 4.5610 | 4.9765 |

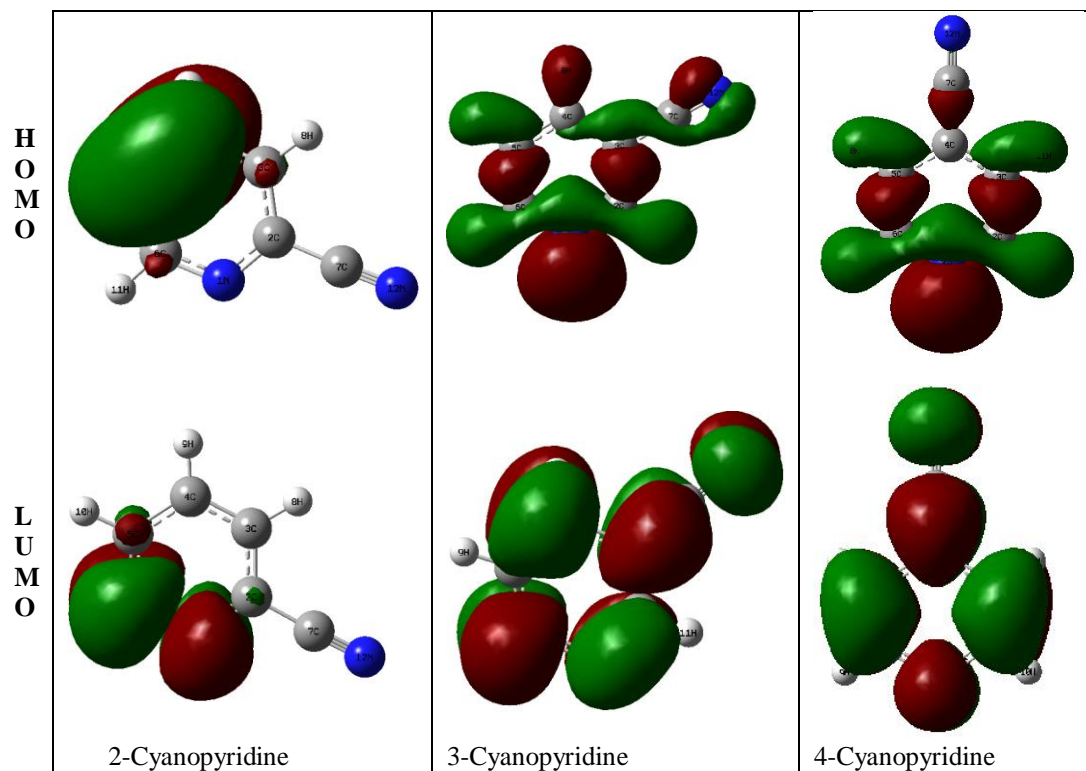


Figure 4. 3D plots of HOMO (top) and LUMO (bottom) orbital of 2-, 3-, and 4-cyano pyridines computed at B3LYP/6-311++G(d,p) level.

3.4 Molecular Electrostatic Potentials and Atomic charges

Atomic charges' calculation plays an important role in the applications of quantum chemical calculations to the molecular system because atomic charges affect molecular properties such as dipole moment, polarizability, and electronic structure. The charge distributions calculated by Mulliken method for the optimized geometries of the three cyanopyridines are listed in Table 7. The result shows that the positive charges are mainly localized on hydrogen atoms, while the carbon atoms are found to be either positive or negative. The cyano group nitrogen atoms (N_{12}) are found to be more negative than the pyridine ring nitrogen atoms (N_1) for all the three isomers. This implies that the cyano group nitrogen is more nucleophilic than the pyridine nitrogen.

Table 7: The Mulliken atomic charges of the optimized structures of 2-, 3- and 4-cyano pyridines.

| Atom No. | Mulliken atomic charges | | |
|----------|-------------------------|--------|--------|
| | 2-CNP | 3-CNP | 4-CNP |
| N_1 | 0.047 | -0.019 | -0.041 |
| C_2 | 0.471 | -0.545 | -0.382 |
| C_3 | 0.391 | 1.743 | 0.038 |
| C_4 | -0.443 | -0.069 | 1.496 |
| C_5 | 0.156 | 0.110 | 0.041 |
| C_6 | -0.228 | -0.326 | -0.382 |
| C_7 | -0.990 | -1.541 | -1.387 |
| H_8 | 0.222 | 0.208 | 0.207 |
| H_9 | 0.189 | 0.189 | 0.185 |
| H_{10} | 0.193 | 0.192 | 0.185 |
| H_{11} | 0.197 | 0.229 | 0.206 |
| N_{12} | -0.204 | -0.170 | -0.167 |

Molecular Electrostatic Potential (MEP) is very important in the study of molecular interactions, prediction of relative sites for nucleophilic and electrophilic attack, molecular cluster and prediction wide range of macroscopic properties [39, 40]. The 3D plots of the molecular electrostatic potentials were calculated by

using the optimized molecular structures at B3LYP/6-311++G(d,p) level for the three cyanopyridines. The results are illustrated in Figs. 5-7. The electrostatic potentials at the surface are represented by different colors; red, blue and green represent the regions of negative, positive and zero electrostatic potentials respectively. In addition, the negative regions (red color) of MEP are related to electrophilic reactivity, and the positive regions (blue color) are related to the nucleophilic reactivity. As can be seen from Figs. 5-7, the negative electrostatic potentials are localized over the nitrogen atoms of the cyano group (CN) and the pyridine ring, and are potential sites for electrophilic attack. The positive regions are localized around the hydrogen atoms.

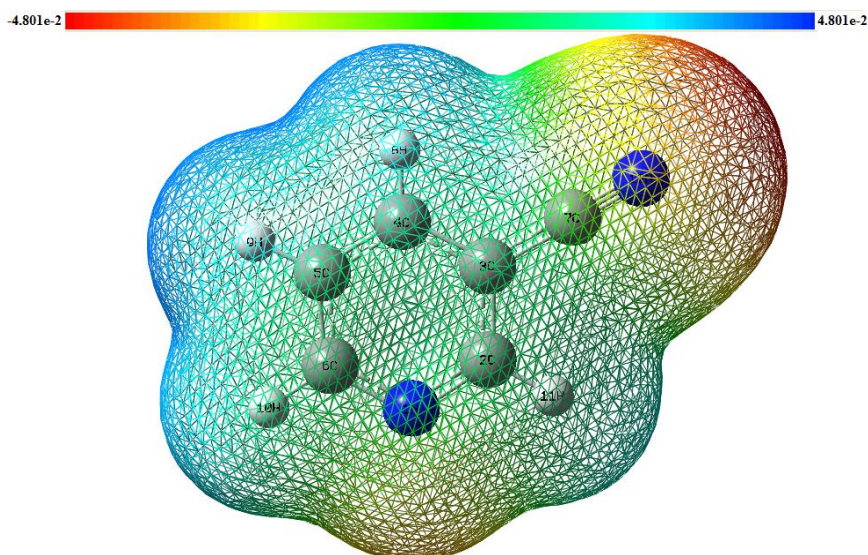


Figure 5. Molecular electrostatic potential energy surface (MEP) for 2-Cyanopyridine

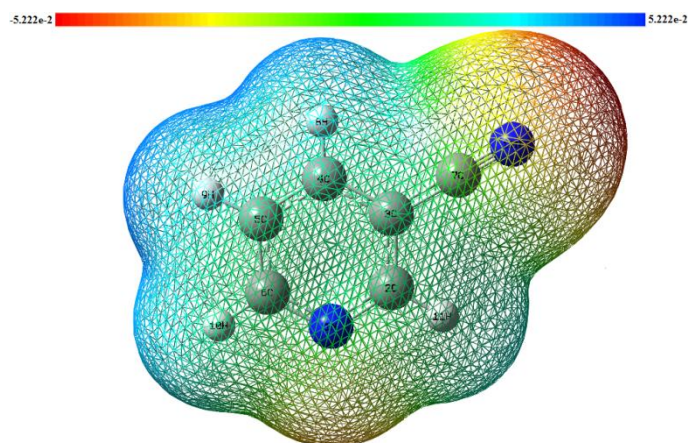


Figure 6. Molecular electrostatic potential (MEP) energy surface for 3-Cyanopyridine

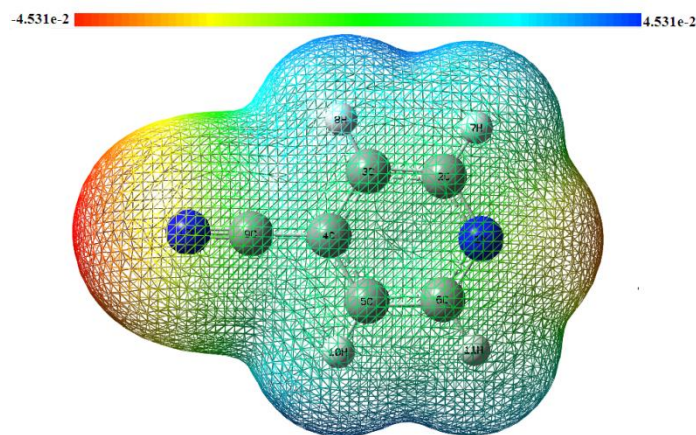


Figure 7. Molecular electrostatic potential (MEP) energy surface for 4-Cyanopyridine

IV. Conclusion

The theoretical structures of three isomeric compounds of cyanopyridines were determined by using the B3LYP/6-311++G(d,p) level of theory. The calculated geometries of the title compounds are in good agreement with the experimental data obtained from X-ray measurement. The optimized structures were used to calculate the vibrational wavenumber, and a reliable assignment of the vibration modes for the three cyanopyridines is proposed on the basis of potential energy distribution (PED). The RMS values calculated for the scaled vibrational modes clearly show a very good agreement with the available experimental data. The RMS and correlation values between the experimental and vibrational wavenumbers are found to be 16 cm^{-1} and 0.9996, 15 cm^{-1} and 0.9997, 16 cm^{-1} and 0.9996, 13 cm^{-1} and 0.9998 for 2-cyanopyridine, 3-cyanopyridine and 3-cyanopyridine respectively. The position of the cyano group (CN) has no significance on the geometric parameters and vibrational spectra of title compounds. The atomic charges, HOMO and LUMO energies, thermodynamic parameters and molecular electrostatic potentials of the molecules were determined and analyzed. The results presented in this paper indicate that density functional theory is reliable for predicting the molecular structures, vibrational spectra and thermodynamic properties of title compounds.

Acknowledgements

Facilities provided by Jubail Industrial College of Royal Commission for Jubail and Yanbu are gratefully acknowledged. The author is grateful to Mohammed Awwal Saidu for editing the manuscript.

References

- [1]. O. Pai, L. Banoth, S. Ghosh, Y. Chisti, U. C. Banerjee, Biotransformation of 3-cyanopyridine to nicotinic acid by free and immobilized cells of recombinant *Escherichia coli*, *Process Biochemistry*, 49(4), 2014, 655–659.
- [2]. Q. A. Almatawah, D. A. Cowan, Thermostablenitrilasecatalysed production of nicotinic acid from 3-cyanopyridine, *Enzyme and Microbial Technology*, 25 (8–9), 1999, 718–724.
- [3]. T. P. Sycheva, T. N. Pavlova, M. N. Shchukina, Synthesis of isoniazid from 4-cyanopyridine, *Pharmaceutical Chemistry Journal*, 6(11), 1972, 696-698.
- [4]. R. Yıldız, A. Döner, T. Doğan, İ. Dehri, Experimental studies of 2-pyridinecarbonitrile as corrosion inhibitor for mild steel in hydrochloric acid solution, *Corrosion Science*, 82, 2014, 125–132.
- [5]. M. Honda, M. Tamura, Y. Nakagawa, K. Nakao, K. Suzuki, K. Tomishige, Organic carbonate synthesis from CO_2 and alcohol over CeO_2 with 2-cyanopyridine: Scope and mechanistic studies, *Journal of Catalysis*, 318, 2014, 95-107
- [6]. J. Scalbert, C. Daniel, Y. Schuurman, C. Thomas, F. C. Meunier, Rational design of a CO_2 -resistant toluene hydrogenation catalyst based on FT-IR spectroscopy studies, *Journal of Catalysis*, 318, 2014, 61–66.
- [7]. J. R. Allan, P. M. Veitch, The preparation, characterization and thermal analysis studies on complexes of cobalt (II) with 2-, 3-, 4-cyanopyridines, *Journal of thermal analysis*, 27(1), 1983, 3-15.
- [8]. Janczak, R. Kubiak, Synthesis, thermal stability and structural characterization of iron (II) phthalocyanine complex with 4-cyanopyridine, *Polyhedron*, 26(13), 2007, 2997-3002.
- [9]. F. A. Mautner, C. Gspan, K. Gatterer, M. A.S Goher, M. A.M Abu-Youssef, E. Bucher, W. Sitte, Synthesis and characterization of three 5-(4-pyridyl)tetrazolato complexes obtained by reaction of 4-cyanopyridine with metal azides from aqueous solutions, *Polyhedron*, 23(7), 2004, 1217-1224.
- [10]. D. S. Abreu, T. F. Paulo, M. L.A. Temperini, I. C.N. Diógenes, Electrochemical, surface enhanced Raman scattering and surface plasmon resonance investigations on the coordination of cyanopyridine to ruthenium on surface, *Electrochimica Acta*, 122, 2014, 204-209.
- [11]. J. Mauger, T. Nagasawa, H. Yamada, Nitrile hydratase-catalyzed production of isonicotinamide, picolinamide and pyrazinamide from 4-cyanopyridine, 2-cyanopyridine and cyanopyrazine in *Rhodococcus rhodochrous* J1, *Journal of Biotechnology*, 8(1), 1988, 87-95.
- [12]. Y. G. Maksimova, D. M. Vasilyev, G. V. Ovechkina, A. Yu. Maksimov, V. A. Demakov, Transformation of 2- and 4-cyanopyridines by free and immobilized cells of nitrile-hydrolyzing bacteria, *Applied Biochemistry and Microbiology*, 49(4), 2013, 347-351.

- [13]. L. Jin, Z. Liu, J. Xu, Y. Zheng Biosynthesis of nicotinic acid from 3-cyanopyridine by a newly isolated *Fusarium proliferatum* ZJB-09150, *World Journal of Microbiology and Biotechnology*, 29(3), 2013, 431-440.
- [14]. C. Crisóstomo, M. G. Crestani, J. J. García, Catalytic hydration of cyanopyridines using nickel(0), *Inorganica Chimica Acta*, 363 (6), 2010, 1092–1096.
- [15]. S. C. Roy, P. Dutta, L.N. Nandy, S.K. Roy, P. Samuel, S. M. Pillai, V.K. Kaushik, M. Ravindranathan, Hydration of 3-cyanopyridine to nicotinamide over MnO₂ catalyst, *Applied Catalysis A: General*, 290(1-2), 2005, 175–180.
- [16]. J.H.S. Green, D.J. Harrison, Vibrational spectra of cyano-, formyl- and halogeno-pyridines, *Spectrochimica Acta Part A: Molecular Spectroscopy*, 33(1), 1977, 75-79.
- [17]. Chen, D. Yang, J. Lipkowski, Electrochemical and FTIR studies of 4-cyanopyridine adsorption at the gold(111) solution interface, *Journal of Electroanalytical Chemistry*, 475(2), 1999, 130-138.
- [18]. M. Laing, N. Sparrow, P. Somerville, The crystal structure of 4-Cyanopyridine, *Acta. Cryst. B27*, 1971, 1986-1990.
- [19]. R. Kubiak, J. Janczak, M. Śledź, Crystal structures of 2- and 3-cyanopyridine, *Journal of Molecular Structure*, 610(1-3), 2002, 59-64.
- [20]. J. D. Magdaline, T. Chithambarathanu, Vibrational Spectra (FT-IR, FT-Raman), NBO and HOMO, LUMO Studies of 2-Thiophene Carboxylic Acid Based On Density Functional Method, *IOSR Journal of Applied Chemistry*, 8(5), 2015, 6-14.
- [21]. M.V.S. Prasad, N. U. Sri, V. Veeraiah, A combined experimental and theoretical studies on FT-IR, FT-Raman and UV-vis spectra of 2-chloro-3-quinolinecarboxaldehyde, *Spectrochimica Acta Part A: Molecular and Biomolecular Spectroscopy*, 118, 2015, 163-174.
- [22]. Y. Umar, Density functional theory calculations of the internal rotations and vibrational spectra of 2-, 3- and 4-formyl pyridine, *Spectrochimica Acta Part A: Molecular and Biomolecular Spectroscopy*, 71(5), 2009, 1907-1913.
- [23]. Y. Umar, Theoretical investigation of the structure and vibrational spectra of carbamoylazide, *Spectrochimica Acta Part A: Molecular and Biomolecular Spectroscopy*, 64(3), 2006, 568-573.
- [24]. Y. Umar, M.A. Morsy, Ab initio and DFT studies of the molecular structures and vibrational spectra of succinonitrile, *Spectrochimica Acta Part A: Molecular and Biomolecular Spectroscopy*, 66(4-5), 2007, 1133-1140.
- [25]. M. Bakiler, O. Bolukbasi, A. Yilmaz, An experimental and theoretical study of vibrational spectra of picolinamide, nicotinamide, and isonicotinamide, *Journal of Molecular Structure*, 826(1), 2007, 6-16.
- [26]. E. Güneş, C. Parlak, DFT, FT-Raman and FT-IR investigations of 5-methoxysalicylic acid, *Spectrochimica Acta Part A: Molecular and Biomolecular Spectroscopy*, 82(1), 2011, 504-514.
- [27]. M. J. Frisch, et al, Gaussian, Inc., Wallingford CT, 2003.
- [28]. D. Becke, Density-functional thermochemistry. III. The role of exact exchange, *J. Chem. Phys.* 98, 1993, 5648-5653.
- [29]. Lee, W. Yang, R. G. Parr, Development of the Colle-Salvetti correlation-energy formula into a functional of the electron density, *Physical Review B*, 37, 1988, 785-789.
- [30]. M. H. Jamroz, *Vibrational Energy Distribution Analysis: VEDA 4 Program* Warsaw (2004).
- [31]. R. Dennington II, T. Keith, J. Millam, et al. GaussView, Version 3.09. (Semichem, Inc., Shawnee Mission, KS, 2003).
- [32]. M. Tursun, G. Keşan, C. Parlak, M. Şenyel, Vibrational spectroscopic investigation and conformational analysis of 1-heptylamine: A comparative density functional study, *Spectrochimica Acta Part A: Molecular and Biomolecular Spectroscopy* 114, 2013, 668-680.
- [33]. G. Keresztury, S. Holly, G. Besenyi, J. Varga, Aiying Wang, J.R. Durig, Vibrational spectra of monothiocarbamates-II. IR and Raman spectra, vibrational assignment, conformational analysis and ab initio calculations of S-methyl-N, N-dimethylthiocarbamate, *Spectrochimica Acta Part A: Molecular Spectroscopy*, 49(13-14), 1993, 2007-2017.
- [34]. G. Keresztury, J. M. Chalmers, Griffith P R (Eds), *Raman Spectroscopy: theory in Handbook of Vibrational Spectroscopy Vol 1*, John Wiley & sons Ltd New York, 2002.
- [35]. R. G. Ford, The microwave spectra and dipole moments of the cyanopyridines, *Journal of Molecular Spectroscopy*, 58(2), 1975, 178-184.
- [36]. M. Kurt, P. C. Babu, N. Sundaraganesan, M. Cinar, M. Karabacak, Molecular structure, vibrational, UV and NBO analysis of 4-chloro-7-nitrobenzofurazan by DFT calculations, *Spectrochimica Acta Part A* 79, 2011, 1162 – 1170.
- [37]. S. Gunasekaran, R.A. Balaji, S. Kumeresan, G. Anand, S. Srinivasan, Experimental and theoretical investigations of spectroscopic properties of N-acetyl-5-methoxytryptamine, *Can. J. Anal. Sci. Spectrosc.* 53, 2008, 149-160.
- [38]. D. F. V. Lewis, C. Ioannides, D. V. Parke, Interaction of a series of nitriles with the alcohol-inducible isoform of P450: Computer analysis of structure—activity relationships, *Xenobiotica*, 24(5), 1994, 401-408.
- [39]. J.S. Murray, K. Sen, *Molecular Electrostatic Potentials Concepts and Applications*, Elsevier Science B.V, Amsterdam, 1996.
- [40]. L.G. Wade Jr., *Organic Chemistry*, sixth ed., Pearson Prentice Hall, New Jersey, 2006.